Authors' Response: Constructing Fast and Accurate Analytical Models for Wind Turbine Main-Bearings

James Stirling [1], Edward Hart [2], and Abbas Kazemi Amiri [2]
[1]Wind and Marine Energy Systems CDT, EEE, University of Strathclyde, Glasgow, UK
[2]Wind Energy and Control Centre, EEE, University of Strathclyde, Glasgow, UK
Correspondence: James Stirling (j.stirling@strath.ac.uk)

Dear reviewers, we would like to thank you again for taking the time to review our manuscript. Your comments made us realise that important clarifications and additional details were required and so we have re-written a great deal of the paper to ensure much greater clarity and more detail is included with respect to the aims, rationales and models used in this work. Furthermore, we discovered that reference frame related issues had been causing originally reported results to be worse than they actually are. Hence, in the updated manuscript you will see that the new model now brings errors related to the moment-reacting support down from over 20% (without torsional springs) to less than 2% (after addition of torsional springs). All equations and code have been thoroughly scrutinised to ensure no issues remain.

Much of the following is taken from our original responses posted to the interactive discussion on the WES page for this paper. Here those same discussions and details are included, with specific additional information about the changes which have now been made, included in red.

Section 1 contains the response preamble which featured in the original responses to both reviewers. The following two sections then address the comments of the two reviewers respectively and take the following form:

- Reviewer's comment
- Authors' response from interactive discussion
- Authors' changes to manuscript

The marked-up manuscript is appended onto the end of this document and all line number references refer to this version of the updated manuscript.

1 Authors' Response Preamble

Recent work which has demonstrated important and unusual load behaviours in wind turbine main bearings has used simplified analytical representations of the drivetrain. Such simple representations will be necessary if this type of analysis is to be performed for large numbers of load cases, incorporated into fleet wide wind turbine digital twin models, used in wind farm simulation software or as part of industry standard BEM programs such as Bladed or FAST. Analytical models of these type are therefore important and already utilised in some instances. However, to date a detailed assessment of how effectively these models represent wind turbine drivetrain load reaction at the main bearing (including different bearing types) has not yet been carried out and it is therefore important to scrutinise the validity of these models and where they might apply.

Wind turbine drivetrains and main bearings in particular are specific to individual turbine designs, as such we are looking to understand in as much generality as possible how these types of analytical models may be used to represent main bearing load characteristics, without focussing on any one design case (since this would reduce the generality and applicability of results). In order to move in this direction, we have identified a need to work up through the available levels of complexity of modelling, understanding at each stage how one model represents the next in the chain. The benefit of such an approach being that at each stage, whenever a lack of agreement is found (such as in the TRB case of the present paper) small additions to the model can be sought to bring the quality of outputs back towards something which is accurate enough to be useful, while also developing knowledge about which effects can and can't be captured at each level.

In the current paper we are starting with the existing 2-dimensional, orthogonally independent, simply supported models and looking to compare with something closer to representing a real world main bearing in a wind turbine drivetrain. Since the strongest assumptions in the initial models are independence of horizontal and vertical planes (from a load perspective) and simply supported load reactions (no moment reaction, only force), we wish to compare their performance against more realistic models that don't necessarily make these assumptions. A 3-dimensional FE model avoids the orthogonality assumption. With respect to simple vs other support types we want to give the 3D model force reaction capabilities which are closer to those of real main bearings in order to assess when the simple support assumption is valid (and to consider how the simple model might be extended to compensate when it's not valid). Main bearings for wind turbines are known to have two force reaction 'types' in general. Bearings that support forces only and not moments (double row SRBs), and bearings that support both forces and moments (double row TRBs) and so simplified bearing representations are created for the 3D FE model which have these general support behaviours (without being exact models for a specific bearings).

Hence, the overarching research goal of this paper is to answer: Can analytical models be used to effectively evaluate load reaction behaviours for 3-dimensional support configurations with either moment reacting or non-moment reacting behaviours at the main support point? Tackling this question in the current paper demonstrates the validity of existing models for force reactions on the bearing as a 'unit' while also setting the stage for further work with more detailed analytical and FE model comparisons which, for example, could start evaluating internal load distributions etc.

- The text of the paper has been extensively revised to ensure the points made in this discussion are very clear throughout the manuscript. In particular, this includes important improvements to the Introduction, Background and FE Model sections, as well as the inclusion of a new Discussion section at the end of the manuscript.

2 Authors' Response to Reviewer 1

1. The authors present a manuscript that deals with the calculation of main bearing re- action forces, based on previous work. They show in a very qualified way how simple approaches can also be used in the wind community. As in previous publications of the authors, the realistic wind conditions, which are used for the calculations, should be emphasized. The manuscript is well organized and written but needs major revisions in both the theoretical and practical areas.

- We agree that a better description of the simulated wind files would help strengthen this paper. We will therefore include this in the updated manuscript and also add extra comments throughout the body of work emphasizing that the outcomes are related to realistic wind conditions and that the models remain effective over a wind turbines full operational range.

- The description of the wind fields used in the study has been updated and expanded and can be found in lines 98-111.

2. The presented results are not repeatable. Concerns arise about the used stiffness values and the practical relevance of the paper. For the FE-models, stiffness values from ROMAX are used, but not named. The authors should give all numbers (including stiffness's, L1 and L2). Furthermore, the dimensions of the used bearing design are interesting for the reader. Since the main shaft will affect the FE-simulations as well, more details are needed.

-We agree that disclosing all dimensions and parameters of the models will help the reader gain a better understanding of the work, as well as improve reproducibility. We have spoken to industry partners and they have given the go-ahead to disclose all parameters in the paper so these will be included in the updated manuscript. A table will also be included to the paper which provides specific input forces and output results for all of the models, further helping the reader to gain an understanding of the behaviour of the models and also to aid in repeatability.

-All model parameters have been included in Table 1. A table has also been included in Appendix A containing hub loading inputs and corresponding model outputs at various time steps.

3. The paper compares a single main bearing system with a SRB and a TRB. It is needless to say, that different bearings need different design of the system and will have different stiffness values. The authors choose an equal design and equal values for SRB and TRB. More and detailed information are needed and a better visualization would be beneficial. The system in Figure 1 shows an axial spring, what does this spring represent?

- This comment is mainly addressed in the introduction of the response and centres around the goals of the study. The main purpose of the study was to compare the accuracy of the analytical models previously published by comparison with more realistic 3-dimensional models, and also test the performance when a different force reaction behaviour is present (i.e. in the case of a TRB). The models are, therefore, deliberately general and do not seek to represent any particular bearing specifically, but rather the global behaviour of different bearing types. Likewise, the rest of the drivetrain system such as the shaft and gearbox connections remain both general and similar for the two different bearing types to create a like for like study on how the bearing behaviours affect the reaction forces seen and our ability to reproduce them with simple analytical models. We agree that the reader's understanding of the work and the FE models would be greatly improved by the inclusion of more detailed illustrations of the FE models and these will be included in the updated manuscript. We also agree that the paper would be improved through a more detailed description of the FE models and will, therefore, include information giving all dimensions, details of the mesh and how the mesh was obtained, connection types and contact conditions in the updated manuscript. The axial spring is the stiffness equivalent of the gearbox connection in the axial direction and a description of this will be added to the paper explaining as such. This value was obtained by Onyx Insight through the use of a similar method used in this paper to obtain the equivalent spring stiffnesses in the full FE gearbox model within the Romax software.

- Descriptions of the axial spring are provided in lines 127-128 and 168-172 and the spring stiffness value is included in Table 1. A more detailed description of the FE models has been included in Section 3 and the reasons for their similarities explained in lines 142-151. Figures 2 and 4 have also been added to provide full images of the FE models.

4. The simulation model needs more explanations as well. It is not clear how the shaft affects the results. The description of the manuscript is not appropriate enough to understand the results in detail. Implementing a torsional stiffness for the TRB seems reasonable. Nevertheless, the new approach will only deliver satisfying results, when the stiffness values from FE-simulations are given. This raises the question of the benefits of the new approach, since a simulation model is needed anyhow. Here the authors should show the benefits of the approach more clearly. It would nice to see a few examples with varying stiffness's, to see the impact.

- The descriptions of the FE models will be enhanced with more detail as stated above. A sensitivity analysis regarding shaft thickness is also being undertaken and included in the paper to illustrate the effect of the shaft on the results. Results of this sensitivity analysis obtained thus far indicate low sensitivity to this parameter, an important addition to the work. As stated in the introduction to the response, we are not claiming that our models directly represent a specific WT drivetrain assembly, however, all WTs have a shaft with a given stiffness and we have displayed the bearing reaction force results when this shaft stiffness is varied. Drive shafts tend to be a mostly solid piece of material, although a small hole will run throughout the shaft to allow for wiring to run through. Therefore, in our analysis we are using shaft thicknesses of 100%, 75% and 50% to conservatively cover realistic thickness (and hence stiffness) values.

The focus of this paper was not to deliver a complete and polished tool but to answer the question of "Can analytical models accurately represent the reaction force behaviour of wind turbine main bearings?". The simple models tested and created in this body of work open the door to mass simulations and analysis in short periods of time and, thus, they could be effectively integrated into wind turbine loads simulation and monitoring at farm level during real-time operation. We agree that this could be made clearer in the paper and thus will improve the narrative in the updated manuscript. With respect to the need for an existing FE model, during the design of WT drivetrains a detailed FE model is usually utilised. However, the company or people that do the detailed drivetrain design work, and hence have access to this FE model, will likely not share it with the wind farm operator who (for example) may be looking to develop digital twin models for their fleet. The benefit of our models is that the WF operator can request access to the non-proprietary values of equivalent stiffness values (determined using the FE model) without requiring access to the model itself. This allows for condensing of information into a form which is less commercially sensitive and allows it to be shared more widely. In addition, even where a full-blown FE model were available, it is not computationally viable to run it for each wind turbine across a wind farm where large scale studies or load/damage tracking during operation might be implemented. Furthermore, in existing certified aeroelastic codes (e.g. Bladed and FAST) structural and load analysis specifically requires for simple and fast running models of subcomponents. Models of the type developed here could therefore end up being integrated into these systems whereas FE models are simply not suitable in this context. As such we believe that there is a strong need for the models considered in this study even where an FE model (with low or high resolution) is available. You are quite right though that this discussion needs to appear in the paper in order to demonstrate the practical usefulness of its outcomes. As such this discussion will be added into the updated manuscript.

- A more detailed description of the FE models has been included in Section 3. A sensitivity analysis on shaft thickness was carried out to determine how shaft stiffness affects the simulation results. The sensitivity analysis results are included in Appendix A. Practicalities of this approach (given you need some access to an FE model) are treated in the new 'Discussion' section at the end of the paper.

5. The authors use realistic load conditions, which makes the manuscript particularly interesting for the wind community. However, since models are compared, simple load cases, which for example only consist of a moment or a certain load, should be additionally used. This provides information about the behaviour, which is not clearly explained in the current manuscript (this also increases repeatability).

- A table of inputs for a particular time step and the corresponding output results for each will be included in the updated paper to help improve the reader's understanding of the models behaviours and also improve the works reproducibility.

- Table A1 has been added to Appendix A which provides a variety of hub loading inputs (in orthogonal force and moment components) and the reaction force results for each model.

6. In general, the introduction uses grey literature and does not show the state of the art of wind turbine main bearings. The authors should heavily improve this part of the manuscript and should focus on peer-reviewed literature instead of grey literature. Especially, the statement in line 65-68 is not supported by the grey literature (YAGI and SMALLEY) and by the previous work (HART), and should be changed appropriate.

- We also agree that more literature pertaining to wind turbine main bearings would strengthen this piece of work and this will be included in the updated manuscript. This will include [1-6], below, among others.

With respect to the second part of the comment, if there is a technical inconsistency at this stage we will be very happy to correct. However, we have struggled a little to understand the specific meaning of the comment relating to lines 65-68. It is of our understanding that the current bearing types used for main bearing in the field are most commonly double row SRBs and TRBs. We realise the bearings themselves are double rowed and we'd not added that detail before and hence have changed the sentence in the updated manuscript to include this distinction. Please feel free to respond with more details and we will endeavour to make sure our manuscript is correctly representing the bearings used for this component. We apologise for not understanding you first time round.

- Section 2 has been expanded to include summaries of recent modelling pertaining to wind turbine main bearings in the literature (lines 64-85). The introduction has also been expanded to include a better description of the study and better define the overarching goal. The statement which was previously in line 65-68 has been altered and can now be found in lines 135-140. We hope this clears up the issue here but if not then we'll be very happy to take any further comments into account.

7. The Figures of the RMSE and Reaction Force are well organized. Nevertheless, in Figure 4 and 6 it is recommended to use equal values for the axis for a) and b).

- This has been updated as requested.

- Figures 4 and 6 have been updated accordingly.

3 Authors' Response to Reviewer 2

1. Specific comments: To be repeatable, basic parameters such as bearing dimensions and stiffnesses should be given. This is not consistently done in the manuscript

- Some parameters were initially left out of the paper due to commercial sensitivity. However, we agree that the inclusion of such parameters will help strengthen the paper by increasing repeatability and have spoken to industry partners who have given the go ahead to disclose such information in the updated manuscript. A table has also been included to the paper which provides specific input forces and output results for all of the models to help the reader to gain an understanding of the behaviour of the models and to aid in repeatability.

- All model parameters have been included in Table 1. A table has also been included in Appendix A containing hub loading inputs and corresponding model outputs at various time steps to further aid reproducibility.

2. In general, more detailed illustrations of the FE models would clearly contribute to understanding. In particular, the consideration of the contact conditions and their simplification within the FE-models should be considered in detail

- We agree that the reader's understanding of the work and the FE models would be greatly improved by the inclusion of more detailed illustrations of the FE models and these will be included in the updated manuscript. We also feel the paper would be improved through a more detailed description of the FE models and have, therefore, included information giving all dimensions, details of the mesh and how the mesh was obtained, connection types and contact conditions in the updated manuscript. This will not only help the reader to better understand the work undertaken but will also improve reproducibility.

- More detailed descriptions of the FE models have been included in Section 3. Figures 2 and 4 have also been added to provide full images of the FE models.

3. The elastic behaviour of the bed plate is set rigid. The author should indicate how this simplification affects the results

- We have looked at the relevant literature (e.g., [1]) concerning modelling of the bedplate and agree that the assumptions made in this study should be brought to the reader's attention and we will therefore include a discussion of this point in the updated manuscript.

- The effects of assuming a rigid bedplate have been included in lines 166-167, citing relevant literature.

4. The physical modelling of the main bearings is not comprehensible. It seems that the spherical roller bearing has been replaced by a deformable spherical joint. It remains questionable whether this form of modelling is permissible, since the contact conditions between rolling elements and running surfaces, which varies under load, results in the characteristic non-linear stiffness of the bearing as such. In addition, no statement is made to whether the bearing clearance of the spherical roller bearing is taken into account. It is unclear how the mesh has been obtained. It is said that larger elements are used for the shaft and smaller elements are used around the bearing and bearing housing to increase accuracy at the contact regions. The mesh density is normally obtained by a convergence study. The author should indicate if this was carried out here

- The purpose of this paper was to develop fast and representative models that can accurately capture the different behaviours between generic SRB and TRB load reaction behaviours when subjected to complex wind loading. As the study was designed to capture general bearing unit force reactions and not internal loads, the SRB was replaced by a deformable spherical joint. The spherical joint in ANSYS will allow the bearing housing to deformably react forces in the X, Y and Z axes while being able to move freely in the rotational degrees of freedom. This allows the non-moment reacting behaviour of an SRB to be captured in a 3-dimensional model without going into the complexity of modelling individual rollers and hence, the global behaviour is still captured in this model in a general form. The characteristics of this simplification and the implications of it in the modelling will be discussed in the revised manuscript.

Referring back to the opening of the response, the overall goal of this study was to determine if the models in the previous study can accurately represent 3D equivalents. Although internal contact conditions between rolling elements and raceways in SRBs display non-linear stiffness behaviours, the system being modelled in this case reacts only through bedplate forces and not coupled moments and forces (where nonlinear stiffness properties would determine the load 'share' between force and moment reaction contributions). As such, the overall reaction force of the bearing housing required to balance the total system remains the same regardless of internal interactions. Non-linear contact behaviour is certainly important when one is seeking to resolve distributed loads internally, but, in the current study it is the overall reaction forces which are of interest. Internal load distributions will be considered as part of the next stages of future work which will increase model complexity to that level.

Thank you for noticing we have not stated whether or not bearing clearance has been taken into account. In this instance we have assumed that there is no bearing clearance since this parameter is known to drive the internal load distribution, rather than overall reaction force. This point will be added to the updated manuscript.

We also agree that our description of how the mesh was obtained can be much improved. A convergence study was in fact carried out to determine the mesh density and a description of this will be included in the updated FE model description.

- The descriptions of the FE models have been improved and include details on bearing clearance assumptions for both the DSRB and DTRB models and Figure 2 and 4 have been added which display the models in their entirety. A description of how the mesh was obtained is also included in lines 176-178 and 191-194. A paragraph considering bearing contact assumptions with respect to both models has also been included (lines 195-207).

5. Also in the case of the tapered roller bearing, it is not apparent whether the contacts between the raceway surfaces and rolling elements were taken into account in the FE model. It seems as if the bearing was modelled as a piece of solid material. If this would be the case, it would have to be questioned to what extent the translational and torsional stiffness of the main bearing can be represented by the FE model. It is also indicated that the preload of the taper roller bearing is taken into account. The author should indicate how exactly the preload is considered.

The analytical model is enhanced by an torsional stiffnesses of the tapered roller bearing. These stiffnesses are set constant and with that a linear stiffness behavior is indicated. In the case of roller bearings a non-linear stiffness behavior can be assumed (hertzian contact, clearance). The author should evaluate which error must be accepted for this simplification.

- Both of these comments tie into the opening of this response and the main goals of this study. You are correct that the load shared between force and moment reactions within the TRB will be determined by the stiffness behaviour (as was touched on above) in the bearing, however, TRB are known to have only weak non-linear behaviour (with a deflection exponent value of 1.1) and TRBs, along with CRBs, are often approximated as linear in their load response. This type of bearing can therefore be approximated to behave like linear steel sections in the FE model and then, since it is the type of load reaction (forces and moments) rather than any one specific design, we have approximated this with a piece of solid material. This is in-line with the stated goal of the paper outlined in the first part of this response (and to be added very clearly into the revised manuscript) to explore how well analytical models might recreate the loads experienced by a support which reacts both forces and moments. This discussion of the modelling assumptions employed, and their viability should have been included in the original manuscript and so we are very grateful you have brought this oversight to our attention. To be clear, we are not proposing that the FE models we employ here should be used to represent real world TRBs, we are developing a methodology from which someone can use an accurate FE representation of their TRB bearing to develop fast and representative analytical models suitable for use in large numbers of load analysis cases, development of digital twin models across a large turbine fleet or similar applications where computationally expensive FE analysis is not viable. The results of this work demonstrate that, up to the level of models employed here, this can be done for both SRB and TRB reaction behaviour types. With respect to the added torsional springs being linear, under small deformations (such as those present in bearings) a torsional spring is equivalent to a pair of parallel linear springs and hence the fact that TRB contact behaviour is only very weakly non-linear indicates that a linear torsional spring is a reasonable approximation. This point will be revisited in future work where internal forces and deformations are considered as modelling complexity is increased. We will also ensure that the above points are clear in the updated manuscript.

As we are interested in the overall forces and moments, the bearing preload effectively gives further justification for assuming the bearing and housing are a solid piece of material (no clearance) – we'll make this point clearer in the updated manuscript.

- As in the previous response, the descriptions of the FE models have been improved and now include details on bearing clearance assumptions etc. The mentioned additional paragraph discussing bearing contact assumptions also helps clarify some of the points raised here (lines 195-207). The comment relating to pre-loading had been made clearer, it is essentially another justification for zero clearance being a reasonable assumption in the DTRB case (line 183).

6. The author should also add the assignment of stiffnesses K and KR in the figures

- K1, K2 and KR will be added to the figures and the values given in the figure description.

- K1, K2 and KR have been added to all relevant figures and their values given in Table 1 and line 281.

Constructing Fast and Representative Analytical Models of Wind Turbine Main-Bearings

James Stirling [1], Edward Hart [2], and Abbas Kazemi Amiri [2]

[1]Wind and Marine Energy Systems CDT, EEE, University of Strathclyde, Glasgow, UK
[2]Wind Energy and Control Centre, EEE, University of Strathclyde, Glasgow, UK

Correspondence: James Stirling, Wind and Marine Energy Systems CDT, EEE, University of Strathclyde, Glasgow, UK (j.stirling@strath.ac.uk)

Abstract. This paper considers the modelling of wind turbine ~~main bearings~~ main-bearings using analytical models. The validity of simplified analytical representations used in existing work is explored by comparing ~~main bearing~~ main-bearing force reactions with those obtained from higher fidelity 3D finite element models. Results indicate that there is good agreement between the analytical and 3D models in the case of a ~~non moment-reacting case~~ non-moment reacting support (such as for ~~a spherical roller bearing~~double row spherical roller bearings), but, the same does not hold in the moment reacting case (such as for double row tapered roller bearings). Therefore, a new analytical model is developed in which moment reactions at the ~~main bearing~~ main-bearing are captured through the addition of torsional springs. This latter model is shown to significantly improve the agreement between analytical and 3D models in the moment reacting case. The new analytical model is then used to investigate load characteristics, in terms of forces and moments, for this type of ~~main bearing~~ main-bearing across different operating points and wind conditions.

1 Introduction

Wind energy provides an important and growing contribution to the European energy market, with 205GW installed as of 2019 - accounting for 15% of consumed electricity (Wind Europe, 2020). As part of this growth, more wind farms are being planned and constructed offshore to take advantage of higher wind speeds and more available construction space (Junginger et al., 2004). Recent trends show dramatic falls in the cost of offshore wind, as been mirrored in the UK's contract for difference auctions which have seen prices drop to £57.50/MWh (UK Government, 2017) and even lower.

With turbines moving further offshore and a need to bring costs down~~means that~~ , reducing operation and maintenance costs, which can be as high as 35% of the total lifetime costs of a project, is becoming increasingly important for wind farm operators (Sinha and Steel, 2015). This in turn effects technology design and selection and puts pressure on original equipment manufacturers (OEMs) and operators to improve turbine reliability. As such, reliability and failure rate considerations have received much attention in the literature ~~(Walford, 2006; Tavner et al., 2007; Wilkinson, 2011)~~(Tavner et al., 2007; Wilkinson, 2011; Artigao et al.,
.

One turbine component with relatively high ~~failures~~ failure rates and associated downtime is the ~~main bearing~~ main-bearing (MB). MBs are becoming recognised as an important component for which failures need to be better understood and reliability improved ~~(Keller et al., 2016; ?)~~(Keller et al., 2016; Hart et al., 2020). MB failure rates have been reported as being ~~up to~~ as high as 30% (Hart et al., 2019) across a 20 year lifetime, with some wind farms having reported MBs failing in less than 6 years (Sethuraman et al., 2015). Recent work which has demonstrated important and unusual load behaviours in wind turbine MBs (Hart et al., 2019; Hart, 2020) implements simplified analytical representations of the drivetrain. Such representations are necessary if this type of analysis is to be performed across large numbers of load cases, incorporated into fleet wide modelling, or into industry standard simulation software (e.g. Bladed and Fast). These types of analytical models are therefore important and already being utilised and, as such, a detailed assessment of how effectively they represent wind turbine drivetrain load response at the MB for different bearing types is an important next step in their development.

~~Preventing premature failures of main-bearings would therefore be an important contribution to reducing operating costs of wind farms. As part of analyses which try to understand the loading conditions of MBs in wind turbines (in order to better understand their operational conditions and load characteristsics), detailed model-based investigations are required. Work of this type exists in the literature (Hart et al., 2019) in which analytical models are used to consider MB loading.~~

Wind turbine drivetrains and MBs in particular are specific to individual turbine designs. As such, it is beneficial to understand in as much generality as possible how existing simple representations may be used to study MB load response, without focusing on any design case (since this would reduce the generality of results). In order to move in this direction, it is necessary to work through levels of modelling complexity, understanding at each stage how well a given model represents the next in the chain. This approach also develops knowledge about which effects can be adequately captured at a given level of model complexity, helping inform decisions with respect to model selection for specific applications.

This paper considers ~~the validity of simplified analytical drivetrain representations of the type used in these load studies by comparisons with higher fidelity~~ an important step in the overall modelling chain; starting with existing 2D, orthogonally independent, simply supported models and looking to compare with higher fidelity models which are closer to representing real-world wind turbine MBs. The strongest assumptions in the existing models are: independence of horizontal and vertical planes (from a load perspective) and simply supported load reactions (i.e. the bearing does not support moment loads). Therefore, this work seeks to compare their performance with more realistic models that remove one or both of these assumptions. More explicitly, 3D ~~finite element models .~~ finite-element (FE) modelling removes the 2D and orthogonality assumptions. With respect to simple versus other supports, MBs for wind turbines have two 'types' of reaction behaviour in general; those that support forces only and not moments (e.g. double row spherical roller bearings (DSRBs)), and those that support both forces and moments (e.g. double row tapered roller bearings (DTRBs)). 3D FE models will therefore be considered which have reaction behaviours that emulate each of the two types. Hence, the overarching goal of this paper is to explore the question:

Can analytical models be used to effectively evaluate load reactions for 3-dimensional main-bearing support configurations with either moment reacting or non-moment reacting behaviours?

Section 2 ~~provides a description of the~~ summarises previous work undertaken in this area. Section 3 then introduces the higher fidelity 3D models which will be used to ~~validate the analytical models before presenting~~ compare with analytical model outputs. Section 4 presents the results of the comparison~~. In section 4~~ , with Section 5 then extending the analytical model

~~is adapted~~ to include moment reactions at the MB~~, before comparing the models again. Section 5 applies~~ . In Section 6 the new analytical model is used to study load behaviours for this bearing type. Finally, Section ~~6~~ 7 discusses some practicalities surrounding the application of these models before Section 8 presents the conclusions of this work.

2 ~~Previous Work~~Background

~~A proper understanding of~~ Despite having received less attention than other drivetrain components, there have been a number of high quality research papers which include modelling and analysis of wind turbine MBs. Cardaun et al. (2019) use a multibody simulation model with flexible components in SIMPACK to investigate main-bearing ~~loading requires full consideration of the complex load environment with which the bearing is interacting. This work expands from work completed previously (Hart et al., 2019) in which hub loading time histories were generated using multi-body aero-elastic software and injected into simplified 2 dimensional models of realistic MB set-ups to determine MB operational loading.~~ loads for a yawed turbine. It was found that yawed inflow has an asymmetric effect on main-bearing loading and fatigue, with the possibility of either increasing or decreasing loading and load fluctuations depending on yaw direction relative to inflow. Bosmans et al. (2019) represent the drivetrain system as lumped parameter components in order to keep degrees of freedom low and increase the speed of simulations, bearings are modelled as linear springs. The study showed differences between port-based and 1D-3D nesting models. In this study focus is on the intermediate and high speed shafts and so the MB is not discussed in detail. In Wang et al. (2020b) the MB is modelled within an overall numerical model of the drivetrain using SIMPACK software. The model consists of both rigid and flexible bodies, with bearings modelled as force elements with linear force-deflection relationships. High fidelity FE models of the critical components are developed in ANSYS before modal reduction is used to minimise degrees of freedom for reduced FE bodies in the system. The paper sought to determine 20-year drivetrain fatigue damage and found that the highest fatigue damage is experienced by the upwind MB. Wang et al. (2020a) determine MB loading for the case where a flexible bedplate is included in modelling. Effects on damage equivalent fatigue loads are explored for flexible and rigid bedplate cases. The study concludes that flexibility in the bedplate leads to a reduction in loading and fatigue experienced by MBs when compared to the rigid case. Kock et al. (2019) use high fidelity FE models to investigate MB internal load distributions and contact pressures when considering variations in elasticity about the bearing circumference and clearance values. Their findings indicate that bearing housing elasticity strongly influences the number of rolling elements under load and the maximum forces experienced by rolling elements.

~~A set of~~ In addition to the analyses outlined above, work has also been undertaken in which simple drivetrain representations are used to study general characteristics of MB loads and their relationship to the incident wind field (Hart et al., 2019; Hart, 2020) , with the current paper building directly on these. The first of these (Hart et al., 2019) considered load characteristics for different possible drivetrain configurations and demonstrated sensitivities to both wind field characteristics and drivetrain setup. More recently, work was undertaken in which repeating structures in time-varying MB loading were identified and characterised, with impacts on the loading experienced by bearing rolling elements also studied. As touched upon in Section

1, the benefit of analytical models employed previously is their simplicity and speed, allowing large numbers of load cases to be analysed rapidly in order to seek possible identifiable trends or recurring off-design load events which may require more detailed scrutiny. While practical for such analyses, it is important to consider the accuracy of these models given their inherent simplifying assumptions and the existence of different load reaction behaviours for different bearing types. These accuracy considerations form the focus of the current paper. The single MB model and turbulent wind field simulations from Hart et al. (2019) will be used here. As such, both will be described below in more detail.

Hart et al. (2019) performed a MB load analysis using simulated loading in realistic wind fields. The 3-dimensional turbulent wind fields were generated in ~~DNV-GL's~~ Bladed software using a Kaimal spectrum ~~in accordance with IEC standards and six different wind fields were created for every combination of the selected wind parameters as required for design certification (IEC, 2005)~~to describe the second order wind field statistics. The three parameters ~~focused on were~~ which characterise these wind fields are hub-height mean wind speeds (10, 12, 16, 20m/s), turbulence intensity (TI) (low, medium and high as specified by the IEC (2005)) and shear profile (power law shear exponents of 0.2 and 0.6)~~resulting in a total~~. 6 different wind fields were generated for each combination of these second order statistics using different initial random number seeds as required for design certification (IEC, 2005). The above provides a total number of 144 ~~wind profiles~~ realistic 3D turbulent wind fields spanning a significant range of typical operational conditions. The 6 wind ~~files~~ fields associated with each combination of the parameters will be referred to as common parameter load sets (CPLS). ~~Bladed was then used to run each wind file through fully aero-elastic multi-body simulations of a~~ A 2MW wind turbine was then simulated operating in each of these 10 minute wind fields using DNV-GL Bladed aeroelastic software, with hub loading time series extracted. This resulted in 144 realistic 10 minute hub loading time series for the 2MW wind turbine~~and the~~, and it is these same load files which are used as inputs to models throughout the current paper. These hub loading time series ~~extracted.~~

~~Simple engineering drawings~~ were then applied to simplified models of MB set-ups (the one used in the current paper is outlined below) in order to study MB load characteristics. Drivetrain details were provided by Onyx Insight~~for the study undertaken in Hart et al. (2019) which provide the dimensions of various MB set-ups and included the gearbox connections~~, this included gearbox connections represented as radial and axial ~~spring stiffness values~~linear springs. Three analytical models were ~~then created including~~ defined which included a single main-bearing (SMB) system and two double main-bearing (DMB) systems. The ~~hub loading time series across the full range of wind files were then injected into the models and the bearing reaction forces extracted. The~~ analytical model for the SMB drivetrain configuration is ~~displayed~~ shown in Figure 1 and ~~will form the focus of this paper.~~

this is the case considered here.

The equation system for the SMB drivetrain set-up is statically determinate and can be solved by balancing the moments about the gearbox giving:

$$F = \frac{M + (L_1 + L_2)B}{L_2}. \tag{1}$$

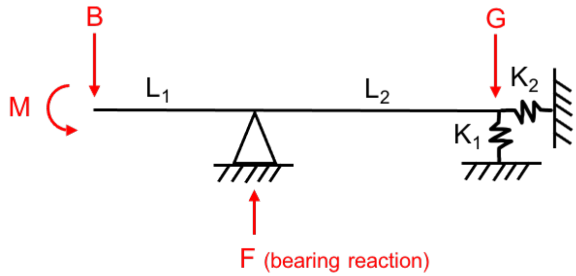

Figure 1. ~~2D analytic~~ Analytic model for single main-bearing set-up in one plane. The full model consists of two such representation, one in each of the horizontal and vertical planes (Hart et al., 2019).

Table 1. Parameters for all models.

Model Parameters	
L_1	2.145m
L_2	2.615m
K_1	8E07N/m
K_2	4E06N/m
G	392280N
Shaft Diameter	0.4m

It is important to note that the overall model consists of two of the type shown in Figure 1, ~~with~~ one in the horizontal and one in the vertical plane, with the resultant force being a vector combination of the two reaction forces at the MB. B and M represent ~~the~~ force and moment loads at the hub ~~,~~ and L_1 and L_2 ~~are 2.145m and 2.615m and~~ represent the distances between the hub and MB, and MB and gearbox ~~,~~ respectively. The axial and radial springs to the right of the model (K_1 and K_2) represent the connection between the shaft and gearbox as stiffness values, while G represents the gearbox ~~mass~~ weight in the vertical plane and is zero in the horizontal plane. F is the ~~bearing support~~ main-bearing reaction force. ~~Findings demonstrated greatly varying mean and peak loads, as well as load ratios, between the different drivetrain configurations and high sensitivities to wind field characteristics~~All model parameters can be found in Table 1.

While models and results in Hart et al. (2019) ~~are promising~~demonstrate potentially important findings, the utilised models are simple, and hence come with limitations. The bearings are modelled as single point fixed supports, meaning all ~~loads are reacted by a reaction force~~ loading is reacted as forces at the MB - with no moment ~~reaction~~ reactions present. The ~~two most~~ model also assumes the independence of loading and reaction behaviour in the horizontal and vertical planes. As outlined in Section 1, two common bearings used for ~~WT MBs are spherical roller bearings (SRB) which cannot react moment loadsand tapered roller bearings (TRB) which can react~~ wind turbine MBs are DSRBs, which cannot support moment loads, and DTRBs, which can support both forces and moments ~~(Yagi, 2004; Smalley, 2015; ?)~~(Yagi, 2004; Smalley, 2015; Hart et al., 2020). Therefore, the validity of existing models ~~for~~ when representing different bearing types ~~should~~ and possible 3D effects is to be considered. ~~This validity is the focus of the current work.~~

3 ~~Comparison of Analytical and FEA models~~Finite Element Models

In order to asses the effectiveness of the simple analytical models used thus far, two ~~finite element (FE)~~ FE models of the SMB system were created in ANSYS~~; with~~ . The FE models were designed to be general and do not seek to represent any particular bearing specifically, but rather the global behaviour of different bearing types; one designed to behave like ~~an SRB,~~ a DSRB (non-moment reacting) and the other to behave like a ~~TRB, as described below~~DTRB (does support moment loads). Likewise, the rest of the drivetrain system such as the shaft and gearbox connections remain both general and similar for the two different bearing types to create a like for like study. The models were subjected to the same hub loading as the analytical models, outlined in the previous section, with bearing support reaction forces outputted and compared with those from the analytical model. Both FE models share dimensions with the SMB analytical model. The FE models themselves still remain relatively simple, with relevant behaviours captured without the modelling of individual rolling elements - as described below. To aid reproducibility a table of input and output value examples for all models is given in Table A1 of Appendix A.

~~SRB~~ DSRB FE Model - The ~~SRB~~ DSRB FE model was created with 3 separate bodies; referred to here as the shaft, the bearing and the bearing housing ~~. A fixed support was added to the base of the bearing housing to represent the connection to the bed plate and the connections between low speed shaft and gearbox was modelled by spring connections horizontally and vertically with stiffness values determined by Romax Technology software.~~ (see Figure 3a). The bearing was connected to the ~~body with a bonded connection and the bearing to bearing housing connection modelled as a deformable~~ shaft using a bonded type contact and the convex outer face of the bearing was connected to the concave inner face of the bearing housing with a spherical joint. This type of connection allows the ~~transfer of force loads from the shaft to the bearing and housing but will not react moments, emulating SRB behaviour . A~~ bearing housing to deformably react forces in the horizontal, vertical and axial axes while being able to move freely in the rotational degrees of freedom, allowing the non-moment reacting behaviour of a DSRB to be captured without the complex modelling of individual rollers. The full model is displayed in Figure 2 and a sliced view of the bearing, housing and shaft can be seen in Figure 3a side-by-side with SRB elements overlaid on the same image to demonstrate the interface type being represented. ~~The mesh was sized to have larger element sizes across the shaft with smaller elements around~~ Bearing clearance is assumed to be zero since this parameter most directly influences the internal load distribution, rather than overall reaction force. The bedplate is assumed to be rigid in this model which, from previous work (Kock et al., 2019; Wang et al., 2020a), can be expected to provide conservatively higher bearing unit reaction force results than if bedplate flexibility were included[1]. A fixed support was added to the base of the bearing housing to represent the connection to the bed plate and the connection between the low speed shaft and the gearbox was modelled by three body-to-ground spring connections in the horizontal, vertical and axial directions. Appropriate equivalent stiffness values

[1] This additional aspect of modelling will be considered in future work as progressively more complex representations are implemented.

of the low speed shaft to gearbox connections were determined with the use of Romax Technology software. The stiffness values, along with model dimensions, can be found in Table 1. The shaft, along with the rest of the model, was designed to be general and is modelled as a solid piece of material. Actual wind turbine main shafts tend to be a mostly solid piece of material, although a small hole will run throughout the centre to allow for wiring to pass to the hub. A sensitivity analysis was therefore undertaken to determine the effect shaft thickness has on results, this can be found in Appendix B, findings indicate low sensitivity to this value. A convergence study was undertaken to determine appropriate mesh densities, resulting in smaller elements on the bearing and ~~bearing housing to increase accuracy at the contact regions.~~ housing bodies and larger elements on the shaft. Input hub loading was applied to the front face of the shaft, the gearbox weight was applied to the rear of the shaft in the vertical axis and main-bearing reaction forces extracted from the fixed support at the base of the housing.

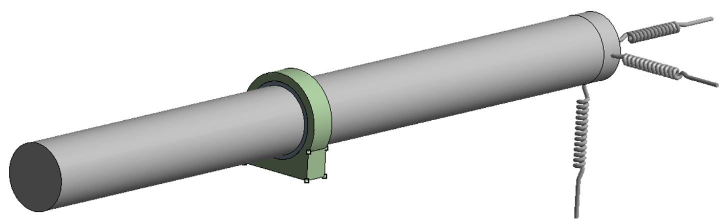

Figure 2. ~~(a) A split view of the SRB FE~~ The 3-dimensional finite element model ~~displaying the geometries of the~~ with double row spherical roller bearing ~~and housing~~type reaction behaviour.~~(b) A split view of the TRB FE model displaying the geometries of the bearing and housing.~~

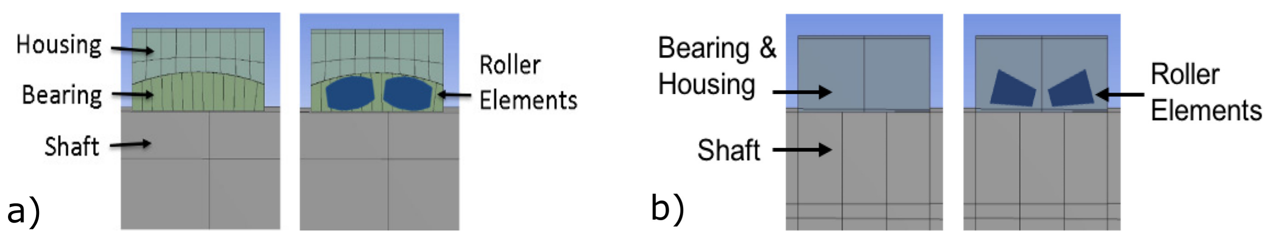

Figure 3. (a) A split view of the SRB FE model displaying the geometries of the bearing and housing. (b) A split view of the TRB FE model displaying the geometries of the bearing and housing. Note: The roller elements and mesh displayed in these images are for illustrative purposes only, a finer mesh was used for the simulations.

~~TRB~~ DTRB FE Model - The ~~TRB~~ DTRB FE model was created with two separate bodies; referred to here as the shaft and the bearing/bearing housing (see Figure 3b). The bearing~~and bearing housing were modeled~~ /bearing housing was modelled as one piece of material ~~with a bonded connection~~ and connected to the shaft using a bonded type contact. This assumes zero clearance between the rollers and housing (typically found in pre-loaded DTRBs) and allows the bearing unit to emulate the force and moment reaction properties of a ~~TRB and the preloading of rollers. A cross section of the~~ DTRB. The dimensions of the model, assumptions of a rigid bedplate and fixed support connection from the base of the bearing/bearing housing to the bedplate are the same as that outlined above in the DSRB description. The low speed shaft equivalent connection to the gearbox and applications of hub and gearbox loading are also the same as described above. The full model is displayed in Figure ~~3b. The base of the~~ 4 and a sliced view of the bearing/bearing housing and shaft can be seen in Figure 3b side-by-side with TRB elements overlaid on the same image to demonstrate the interface type being represented. Model parameters can be found in Table 1. The shaft was again modelled as a solid piece of material. Sensitivity analysis results for this configuration, relating to shaft thickness, can also be found in Appendix B. A convergence study was again undertaken to determine appropriate mesh densities. The DTRB main-bearing ~~housing was modelled with a fixed support to represent the connection tothe main bed plate and the gearbox was again modelled by body-to-ground horizontal and vertical spring connections with the same stiffness properties as the SRB model~~ reaction forces were extracted from the fixed support at the base of the housing.

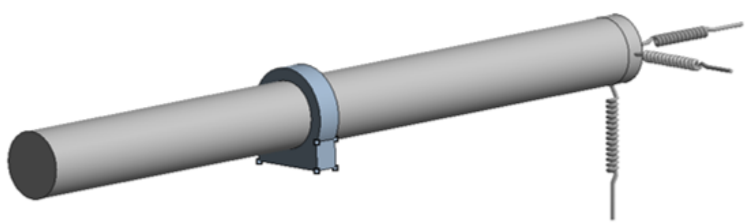

Figure 4. The 3-dimensional finite element model with double row tapered roller bearing type reaction behaviour.

Bearing contact assumptions: Internal contact conditions and load distributions around the bearing circumference are important (and non-linear) aspects of bearing behaviour. However, the SMB analytical model being studied is not designed to go to this level of detail - instead outputting the reaction forces at (or equivalently the loads applied to) the MB. As such, the simplified FE representations for DSRB and DTRB bearings outlined above are considered reasonable for the following reasons: DSRB case - DSRBs are self-aligning and hence provide force but not moment reactions across the bearing, as such, the reaction force required to balance the system should remain the same irrespective of the spring properties, with only displacement magnitudes effected, since the system is determinate. DTRB case - in the DTRB case the system supports moments through opposite force reactions over the two bearing rows in addition to providing an overall force reaction. Consequently, nonlinear contact properties of the rollers will influence the share between force and moment reactions at the MB. However, the non-linearity present in line contact rollers[2] is only slight, with an exponent of 1.11 (Harris, 2006), and so they are reasonably approximated as linear (Dowson and Higginson, 1977; Tibbits, 2005). Considering the research question posed in Section 1, it is therefore argued that the FE DTRB model presented here sensibly recreates load reaction behaviours of the desired type.

~~Plots of~~

[2] Including tapered and cylindrical cases.

4 Comparison of Analytical and Finite Element Models

The analytical model presented in Section 2 was compared with the FE models described in Section 3 to determine its validity when the 2D orthogonality and simply-supported reaction assumptions are removed. The models were compared by performing a root mean squared error (RMSE) ~~comparison results~~ analysis between the reaction force results for the models across the whole range of turbulent wind field load time histories. Plots of RMSE between the analytical and two FE models are shown in Figures 5 and 7, along with example time series plots of ~~the bearing unit~~ MB reaction forces in Figures 6 and 8. The RMSE plots present the mean and standard deviations ~~from~~ within each CPLS (which each capture results from 6 wind files with parameters in common) with respect to mean wind speed, turbulence intensity and shear profile. Note that mean wind ~~speeds~~ speed values are staggered for clarity.

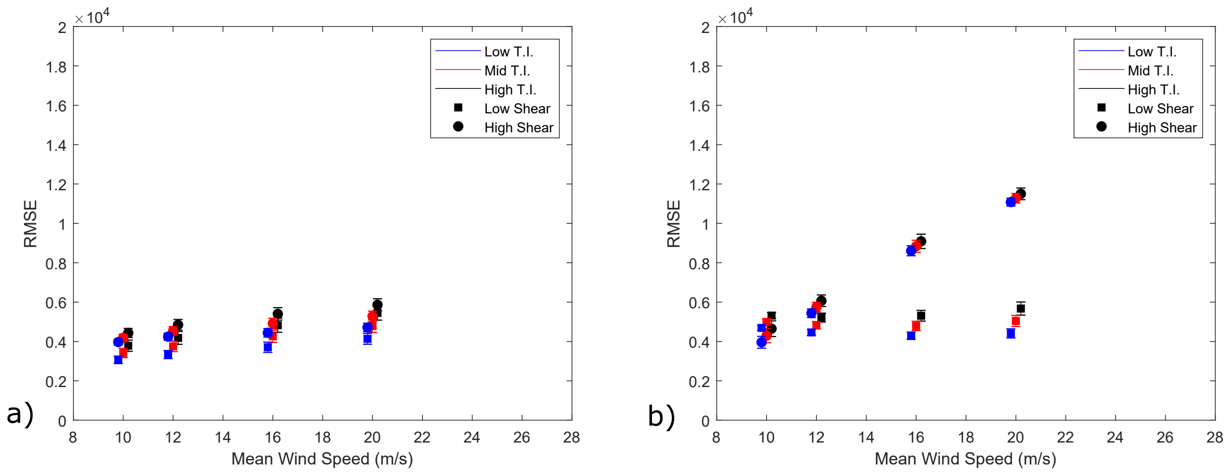

Figure 5. (a) RMSE between reaction forces from the analytical and ~~SRB~~ DSRB FE model in the ~~horizontal plane~~**horizontal plane**. The mean and standard deviations within each CPLS are plotted, staggered about mean wind speed for clarity. (b) RMSE reaction force results between the analytical and ~~SRB~~ DSRB FE model in the ~~vertical plane~~**vertical plane**. The mean and standard deviations within each CPLS are plotted, staggered about mean wind speed for clarity.

Figure 5 displays RMSE results between the analytical model and the ~~SRB~~ DSRB FE model in the horizontal and vertical planes. The accuracy of the analytical model in the horizontal axis appears to have slight sensitivities to wind speed and shear exponents, decreasing as their values increase. The RMSE results for the bearing reaction force in the vertical axis are more differentiated by the varying wind parameters than in the horizontal axis. The low shear results remain fairly constant with increasing wind speed, although increasing sensitivity to ~~T.I.~~ TI with increasing wind speed can be seen. The high shear exponent results ~~appear to be very~~ are more sensitive to wind speed with RMSE values increasing with wind speed. To put these results into context, the mean percentage error between resultant force magnitudes for the two models across all wind files is 1.54%, with a mean correlation coefficient of 0.9996. These results indicate that the analytical model does in fact give good results across all tested wind profiles in both planes when compared with 3D model outputs. This conclusion is reinforced when one considers time series of these loads, with examples shown in Figure 6.

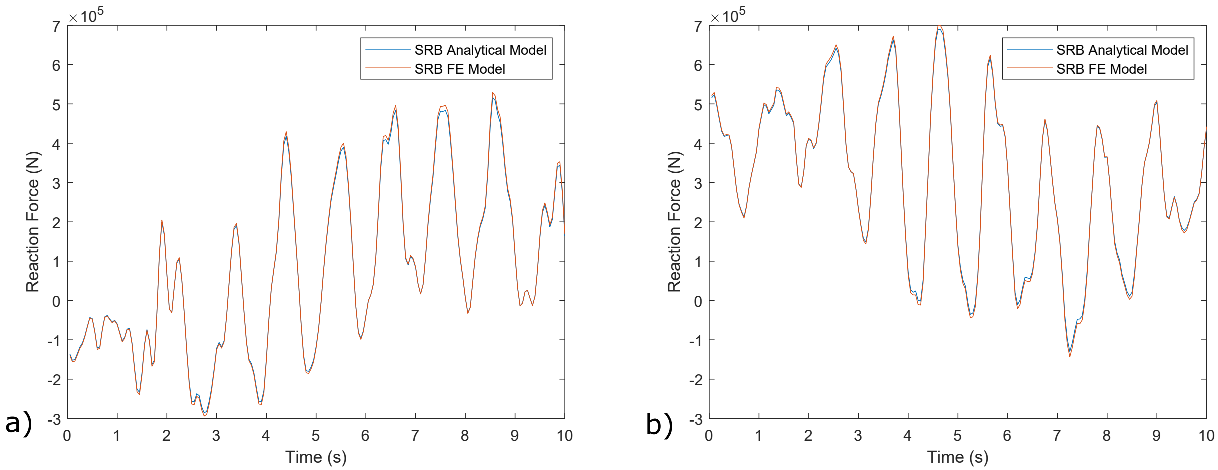

Figure 6. (a) Example time series of reaction force results in the ~~horizontal plane~~ **horizontal plane** from the analytical and ~~SRB~~ DSRB FE models. (b) Example time series of reaction force results in the ~~vertical plane~~ **vertical plane** from analytical and ~~SRB~~ DSRB FE models.

The analytical model reaction force results were then compared with the ~~TRB~~ DTRB FE model, with the results displayed in Figure 7. The analytical model shows a trend of decreasing accuracy with increasing wind speed and shear in the horizontal plane. Compared to the previous results, error values can be seen to have significantly increased by more than a factor of 10. The accuracy of the model in the vertical plane is highly sensitive to wind shear. Increasing mean wind speeds ~~for low shear does not appear to effect~~ and TI slightly decreases the accuracy of the ~~model~~ low shear results in the vertical plane~~, but, sensitivities to turbulence intensity are evident~~. In contrast, the high shear exponent results in the vertical plane significantly decrease in accuracy ~~significantly~~ with increasing mean wind speeds and show less sensitivity to TI. The mean percentage error and correlation coefficient were again considered between resultant force magnitudes across all wind ~~files~~cases. The mean error was found to be ~~31.1~~22.74% and a mean correlation coefficient of ~~0.802~~ 0.7781 was calculated, showing that the analytical model is noticeably less accurate in the ~~TRB moment reacting~~ DTRB, moment-reacting, case. This conclusion is again reinforced by time series of model outputs, examples of which are shown in Figure 8.

The ~~comparison results between the analytical and FE models suggests that~~ above comparisons suggest the orthogonal independence and simple support assumptions made in the analytical model ~~is generating~~ still allow for valid force outputs ~~in the SRB case~~when representing a DSRB. However, the results also show that the analytical model ~~cannot accurately represent~~ has significantly overestimated the force reactions for ~~a TRB~~ the DTRB system. This motivates the derivation of a new analytical model ~~in order~~ to try and emulate the positive results seen in the ~~SRB for a TRB setup~~DSRB case for moment reacting DTRBs. Such a model is developed in the following section.

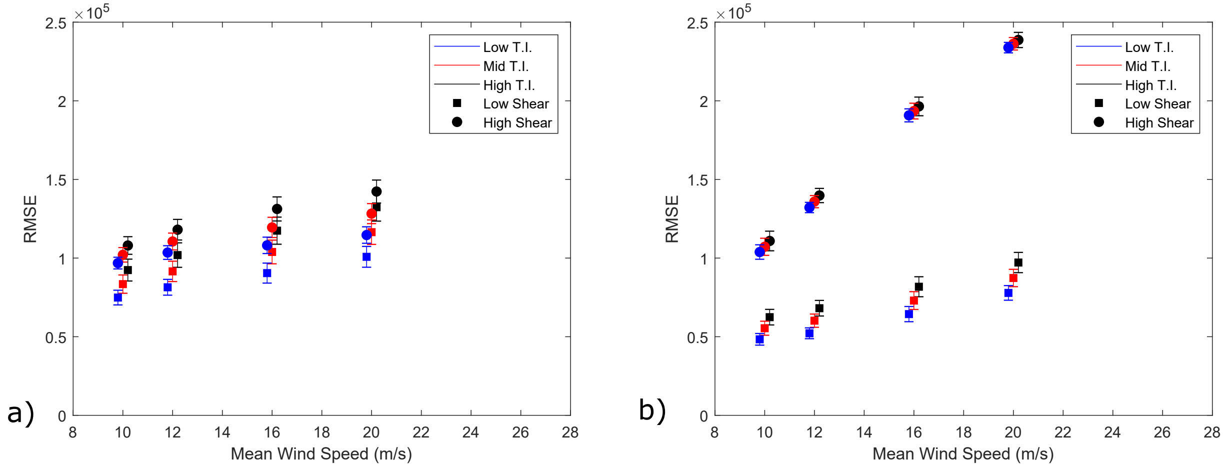

Figure 7. (a) RMSE between reaction forces from the analytical and ~~TRB~~ DTRB FE model in the ~~horizontal plane~~**horizontal plane**. The mean and standard deviations within each CPLS are plotted, staggered about mean wind speed for clarity. (b) RMSE reaction force results between the analytical and ~~TRB~~ DTRB FE model in the ~~vertical plane~~**vertical plane**. The mean and standard deviations within each CPLS are plotted, staggered about mean wind speed for clarity.

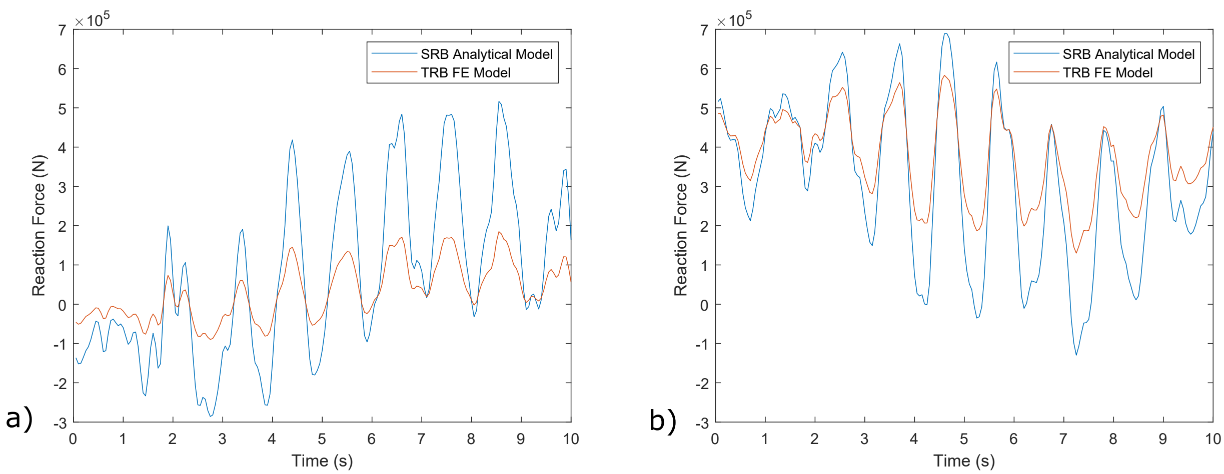

Figure 8. (a) Example time series of reaction force results in the ~~horizontal plane~~ **horizontal plane** from the analytical and ~~TRB~~ DTRB FE models. (b) Example time series of reaction force results in the ~~vertical plane~~ **vertical plane** from analytical and ~~TRB~~ DTRB FE models.

5 ~~Adapting~~ Extending the ~~analytical model for moment reactions~~Analytical Model to Include Moment Reactions

In order to ~~facilitate~~ allow moment reactions at the MB, torsional springs were added to the fixed bearing support in both planes of the analytical model. Thus, a new analytical model was created, displayed in Figure 9~~(a)~~a. The set of equations for the new

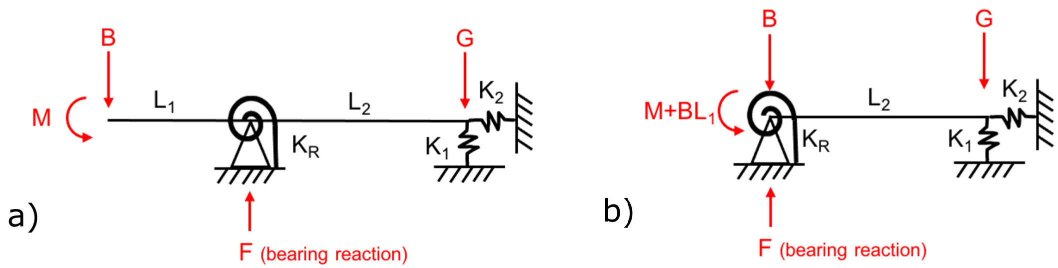

Figure 9. (a) ~~2D analytical~~ Analytical model for single main-bearing ~~set-up~~ setup with torsional spring to include moment reactions. The overall model consists of one in the horizontal and one in the vertical plane. (b) Simplified ~~2D~~ analytical model with torsional spring.

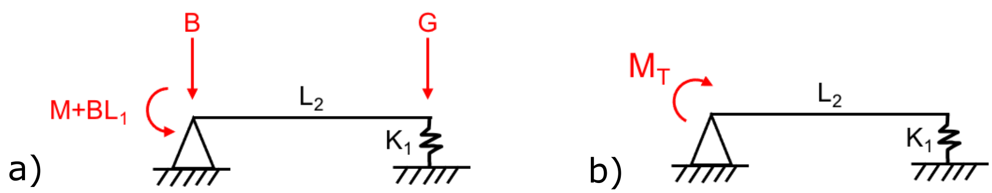

Figure 10. (a) Deflection model 1 (rotor weight and overturning moment). (b) Deflection model 2 (torsional spring reaction force).

analytical model are statically indeterminate and so the model must be decoupled to find a solution ~~(??)~~(Hibbeler, 2011; K. Leet, C. Uang, 2 . The model was first simplified by moving the location of the force applied by the rotor mass, B, and associated overturning moment, M, to be positioned at the bearing support mount as shown in Figure 9 (b). The model was then decoupled into two deflection models; one which has the rotor weight and overturning moment acting on the structure (Figure 10 (a)) and one which has the reaction moment from the torsional spring acting on the structure (Figure 10~~(b)~~b).

The two deflection models can then be decoupled again to show the two mechanisms causing deflection in the shaft; bending of the beam due to the applied moment, and rotation about the ~~main-bearing~~ MB support due to spring support (gearbox) compression/extension. As the deflection mechanisms and equation derivation process is similar for the overturning moment and spring reaction moment on the system, only the equations and deflection mechanisms for the overturning moment is presented here. The two deflection mechanisms for the decoupled model with overturning moment and rotor weight is shown in Figure 11.

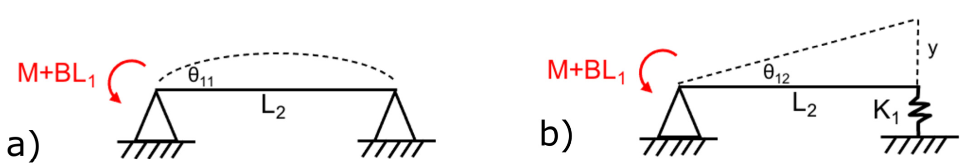

Figure 11. Deflection mechanisms for deflection model 1 under some applied moment $\cancel{M_A}$ $M+BL_1$.

Calculating θ_{11} as seen in Figure 11 can be done by utilising the beam deflection formula shown in Equation 2 (Popov, 1990).

$$\theta_{11} = \frac{(M + BL_1)L_2}{3EI} \tag{2}$$

~~Calculating θ_{12} is not as straightforward as the~~ The compression/extension length, y, of the spring must first be found before calculating θ_{12}. For a loaded spring with stiffness, ~~k~~ K_1, the distance stretched or compressed, y, is equal to the reaction force divided by the stiffness.

$$y = \cancel{\frac{R_B}{k}} \frac{R_B}{K_1}, \tag{3}$$

Trigonometrically, the deflection angle is then,

$$\tan\theta_{12} = \frac{y}{L_2}, \tag{4}$$

and a small-angle approximation simplifies the equation to,

$$\theta_{12} = \frac{y}{L_2}, \tag{5}$$

and ~~so subbing in~~ combining with Equation 3 for y gives,

$$\theta_{12} = \cancel{\frac{R_B}{KL_2}} \frac{R_B}{K_1 L_2}. \tag{6}$$

The second set of deflection equations with respect to the reaction moment of the torsional spring on the shaft are calculated using the same method, with the angles of rotation labelled θ_{21} and θ_{22} and taking values of,

$$\theta_{21} = \frac{M_T L_2}{3EI}, \tag{7}$$

and,

$$\theta_{22} = \cancel{\frac{R_T}{KL_2}} \frac{R_T}{K_1 L_2}. \tag{8}$$

The rotation of the torsional spring, θ_{TS}, is given by,

$$\theta_{TS} = \frac{-M_T}{K_R}, \tag{9}$$

where K_R is the stiffness of the torsional spring and M_T the reaction moment. The rotation of the torsional spring is also equal to the sum of all deflection angles, with positive and negative signs indicating direction,

$$\theta_{TS} = -\theta_{11} - \theta_{12} + \theta_{21} + \theta_{22}. \tag{10}$$

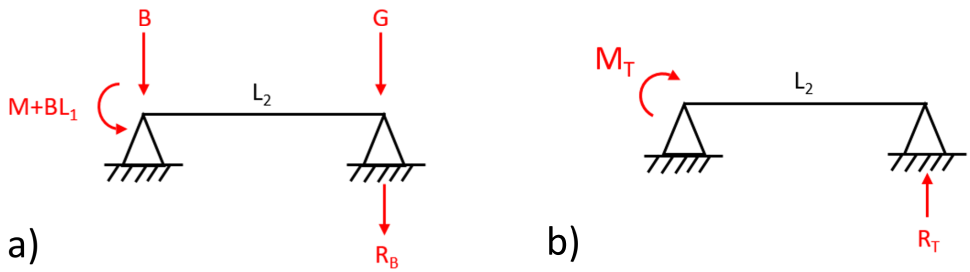

Figure 12. (a) Force balance corresponding to deflection model 1. (b) Force balance corresponding to deflection model 2.

The reaction forces R_B and R_T are still unknowns and the above equation cannot be solved until the forces are balanced on the decoupled models. Balancing the moments about the bearing support in Figure 12~~(a)~~ a gives,

$$-(M + \underline{L}BL_1\underline{B}) + GL_2 + R_BL_2 = 0, \tag{11}$$

from which it follows,

$$R_B = \frac{(M + L_1B) - GL_2}{L_2}. \tag{12}$$

Similarly, moments can be balanced about the bearing support for the decoupled model loaded with the reaction moment from the torsional spring displayed in Figure 12~~(b)~~ b giving,

$$M_T - R_TL_2 = 0, \tag{13}$$

and hence,

$$R_T = \frac{M_T}{L_2}. \tag{14}$$

These expressions for R_B and R_T can now be ~~subbed~~ entered into Equations 6 and 8, respectively, resulting in solvable equations for θ_{12} and θ_{22}:

$$\theta_{12} = \underline{\frac{(M + L_1B) - GL_2}{KL_2^2}}\,\frac{(M + L_1B) - GL_2}{K_1L_2^2}, \tag{15}$$

$$\theta_{22} = \underline{\frac{M_T}{KL_2^2}}\,\frac{M_T}{K_1L_2^2}. \tag{16}$$

Equation 10 can therefore be written in full in terms of known quantities as,

$$-\frac{M_T}{K_R} = -\frac{(M + BL_1)L_2}{3EI} - \underline{\frac{(M + BL_1) - GL_2}{KL_2^2}}\,\frac{(M + BL_1) - GL_2}{K_1L_2^2} + \frac{M_TL_2}{3EI} + \underline{\frac{M_T}{KL_2^2}}\,\frac{M_T}{K_1L_2^2}, \tag{17}$$

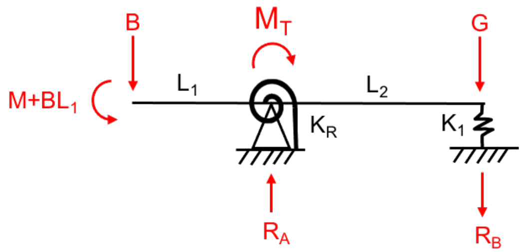

Figure 13. Force balance model for the whole system

and rearranged for M_T as,

$$M_T = \left[\frac{(M+BL_1)L_2}{3EI} + \cancel{\frac{(M+BL_1)-GL_2}{KL_2^2}}\frac{(M+BL_1)-GL_2}{K_1L_2^2}\right]\left[\cancel{\frac{1}{\frac{1}{K_R}+\frac{1}{KL_2^2}+\frac{L_2}{3EI}}}\frac{1}{\frac{1}{K_R}+\frac{1}{K_1L_2^2}+\frac{L_2}{3EI}}\right]. \tag{18}$$

The equation for the reaction moment from the torsional spring, M_T, has ~~now~~ been derived and, as such, the system is now statically determinate. A moment balance can be performed on the gearbox support over the whole system, as shown in Figure 13, to derive the reaction force at the bearing support, R_A,

$$R_A = \frac{M + B(L_1+L_2) - M_T}{L_2}. \tag{19}$$

5.1 Estimating Torsional Spring Stiffness

Having derived the relevant equations for a new analytical model with moment reaction capabilities~~via torsional springs~~, it is then necessary to determine appropriate ~~spring stiffness~~ spring-stiffness values in each plane. These were estimated using the FE ~~TRB~~ DTRB model. The body-to-ground springs representing the shaft connection to the gearbox were removed from the model and four nodes selected: one at the bedplate connection and one at the top of the bearing housing for the vertical plane, and one on both sides of the bearing housing at points of mid height and mid thickness for the horizontal plane. Known moments were then applied about the horizontal and vertical axes separately and the displacement of the nodes recorded. The angle of rotation about the mid point of the vertical nodes ~~could then be~~ was calculated and used to determine the vertical axis spring stiffness via the standard spring equation (Equation 20). Likewise, the angle of rotation about the centre of the housing between the pre and post-loaded nodal points was calculated and the torsional spring stiffness about the horizontal axis estimated. These steps are illustrated in Figures 14 and 15.

$$K = \frac{M}{\theta} \tag{20}$$

The two estimated spring stiffness values, approximately ~~436KN~~392kN/rad in the horizontal plane and ~~104KN~~145kN/rad in the vertical plane, were then applied ~~to the analytical TRB~~ in the analytical DTRB model and the reaction forces at the bearing ~~were~~ calculated across the wind profiles. Examining the time series plots of the reaction forces of the ~~FEA TRB~~ FE DTRB and

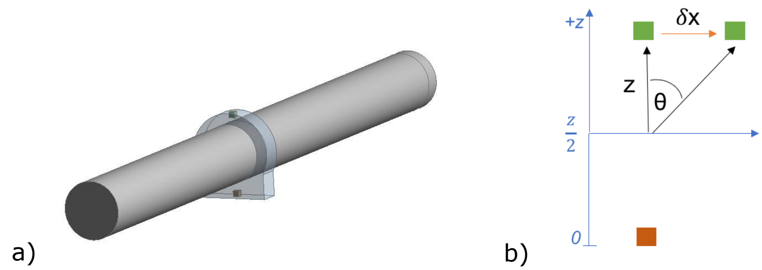

Figure 14. Node selection within the bearing housing for estimating torsional spring stiffness in the vertical plane.

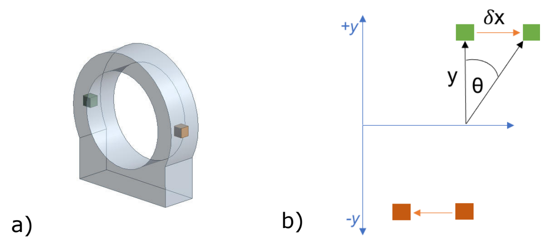

Figure 15. Node selection within the bearing housing for estimating torsional spring stiffness in the horizontal plane.

the analytical ~~TRB models (presented in~~ DTRB models (Figure 17)~~indicates that~~, the new analytical model ~~is capturing well the loading characteristics of the FE TRB model~~ appears to capture the loading seen by the FE DTRB model very closely in both planes.

RMSE results in this case are plotted in Figure 16. It can be seen from the plots that the inclusion of the torsional springs greatly reduces the RMSE values, as well as variance within each CPLS, between the analytical and ~~TRB~~ DTRB FE models in both the horizontal and vertical planes. The mean absolute error and mean correlation coefficients between resultant force magnitudes were calculated for the two models~~, –~~; mean percentage error in this case has dropped to ~~16.54~~1.61% while the mean correlation coefficient has increased to ~~0.9984~~0.9996. The results in Figure 16 show shear profile to have the strongest effect on model accuracy in the vertical plane. It can also be seen that the low shear cases accuracy increases with increasing mean wind speed while high shear cases accuracy decreases with increasing mean wind speed.

6 Investigating mean and peak loads of a SMB with ~~both SRB~~ DSRB and ~~TRB~~DTRB supports

Presented results imply that the analytical SMB model ~~of~~ used in Hart et al. (2019) and the ~~new~~ analytical moment reacting model developed here provide ~~reasonable representations of SRB and TRB setups~~ good representations of DSRB and DTRB type reaction forces (and moments in the latter case) respectively. As where in previous work the mean and peak loads across operating points ~~was~~ were considered, here these same values will be investigated for the ~~TRB~~ DTRB case using the analytical ~~TRB~~ DTRB model, with the original being referred to as the analytical ~~SRB~~ DSRB model.

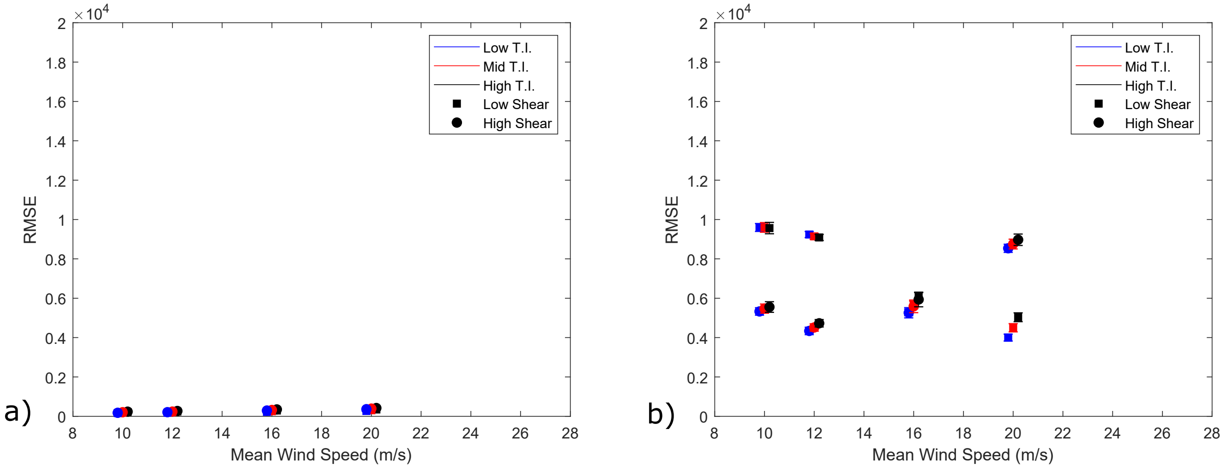

Figure 16. (a) ~~Example time series of~~ RMSE between reaction ~~force results in the horizontal plane~~ forces from the analytical ~~TRB~~ DTRB (with torsional springs) and ~~TRB~~ DTRB FE ~~models~~model in the **horizontal plane**. The mean and standard deviations within each CPLS are plotted, staggered about mean wind speed for clarity. (b) ~~Example time series of~~ RMSE reaction force results ~~in~~ between the ~~vertical plane from~~ analytical ~~TRB~~ DTRB (with torsional springs) and ~~TRB~~ DTRB FE ~~models~~model in the **vertical plane**. The mean and standard deviations within each CPLS are plotted, staggered about mean wind speed for clarity.

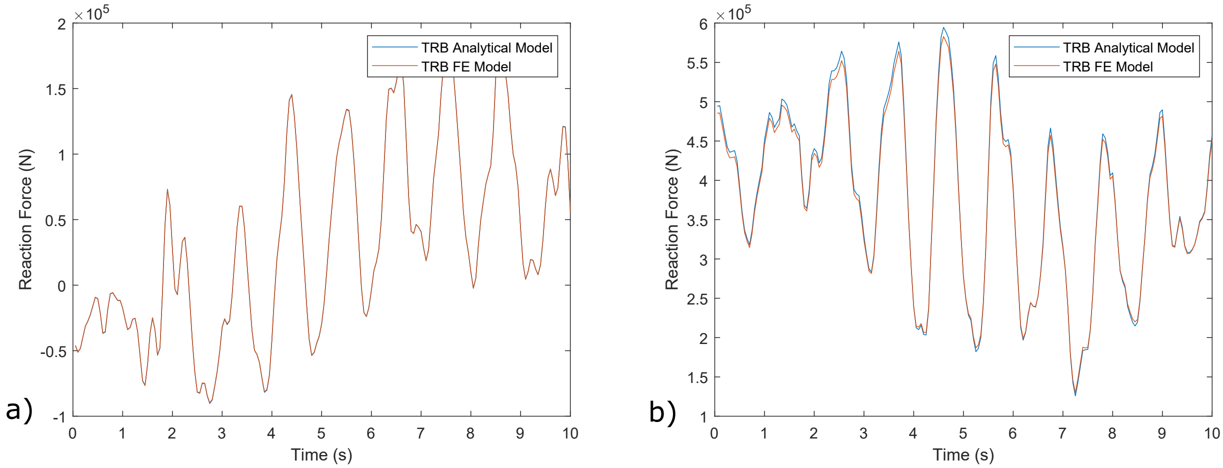

Figure 17. (a) ~~RMSE between~~ Example time series of reaction ~~forces~~ force results in the **horizontal plane** from the analytical ~~TRB~~ DTRB (with torsional springs) and ~~TRB~~ DTRB FE ~~model in the horizontal plane~~models. ~~The mean and standard deviations within each CPLS are plotted, staggered about mean wind speed for clarity.~~ (b) ~~RMSE~~ Example time series of reaction force results ~~between~~ in the **vertical plane** from analytical ~~TRB~~ DTRB (with torsional springs) and ~~TRB~~ DTRB FE ~~model in the vertical plane~~models. ~~The mean and standard deviations within each CPLS are plotted, staggered about mean wind speed for clarity.~~

The mean radial loading for the analytical ~~SRB~~ DSRB model in the previous study showed high sensitivity to shear exponent with the low shear exponent wind files resulting in larger radial loading. ~~The low shear files saw loads~~ Plotted low shear results lay between 400 and ~~500KN and the~~ 500kN, similarly, high shear exponent ~~files~~ plotted results were between around 200 and ~~300KN~~300kN. The mean loads within each CPLS remained fairly constant with small standard deviations and TI had some effect on the results, with higher TI resulting in slightly higher loading.

Mean radial force and moment results for the analytical ~~TRB~~ DTRB model are shown in Figure 18. The presence of moment as well as force reactions can be seen to have reduced the mean radial force loading across the full envelope of wind conditions when compared with results in Hart et al. (2019), while also reducing the system's sensitivity to shear profile. The mean force loads within each CPLS remain fairly constant with small deviations at low mean wind speeds, although deviations increase with increasing wind speeds.

Considering moment reactions, the ~~RMSE values increase~~ magnitude increases with increasing mean wind speeds and the high shear ~~files~~ cases contribute to larger moment loading compared to low shear cases. There are also ~~slight sensitivities to T.I.~~ sensitivities to TI in both shear exponent cases.

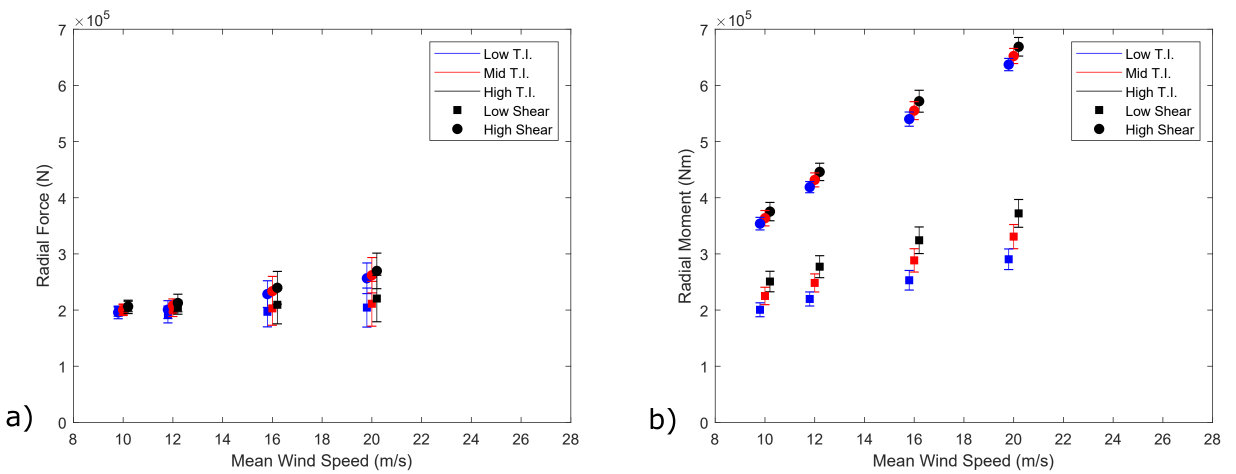

Figure 18. (a) ~~Mean~~ **Mean** radial resultant ~~force magnitudes~~ **force magnitudes** from the analytical ~~TRB~~ DTRB model. Mean and standard deviations within each CPLS are plotted, staggered about mean wind speeds for clarity. (b) ~~Mean~~ **Mean** resultant ~~moment magnitudes~~ **moment magnitudes** from the analytical ~~TRB~~ DTRB model. Mean and standard deviations within each CPLS are plotted, staggered about mean wind speeds for clarity.

The analytical ~~SRB~~ DSRB peak radial loads presented in Hart et al. (2019) show peak loads increasing in size and variability with increasing wind speeds. The peak loads see significant changes with TI but are most sensitive to shear exponent. ~~All the loads fall within 500KN~~ Plotted results fall within 500kN and 1,~~200KN. The~~ 200kN. The plotted mean peak radial reaction forces in the SMB system with a ~~TRB~~ DTRB fall within the range of approximately ~~540KN to 960KN~~ 510kN to 955kN and show a reduced sensitivity to shear exponent as shown in Figure 19. The overall trend of the results displays ~~RMSE~~ magnitude and variability increasing with mean wind speed. The peak moment loads show high overall sensitivity to shear exponent, TI and mean wind speed~~and T. I.~~. The variability of peak moment loads also increases with wind speed.

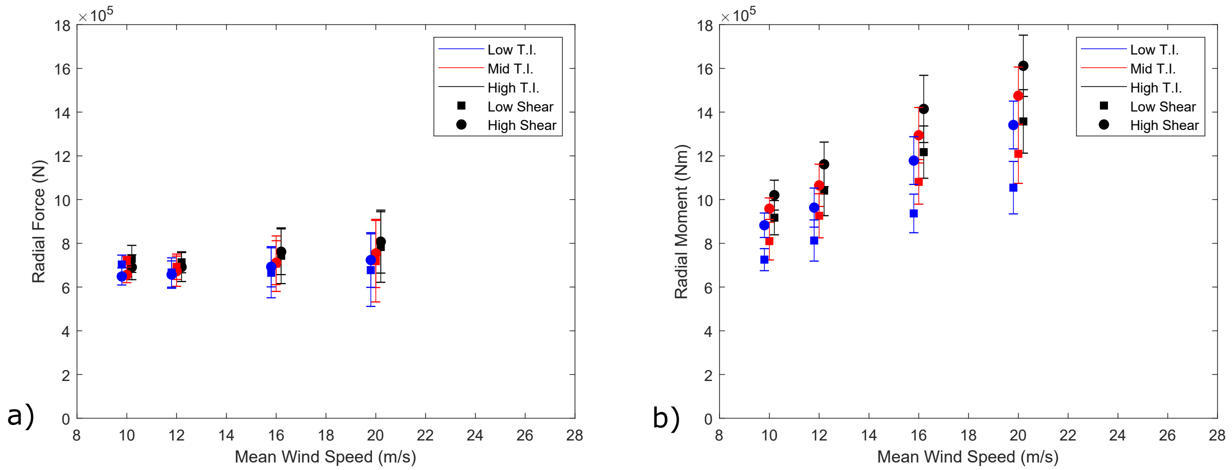

Figure 19. (a) ~~Peak~~ **Peak** radial resultant ~~force magnitudes~~ **force magnitudes** from the analytical ~~TRB~~ DTRB model. Mean and standard deviations within each CPLS are plotted, staggered about mean wind speeds for clarity. (b) ~~Peak~~ **Peak** resultant ~~moment magnitudes~~ **moment magnitudes** from the analytical ~~TRB~~ DTRB model. Mean and standard deviations within each CPLS are plotted, staggered about mean wind speeds for clarity.

7 Discussion

The previous sections have outlined how the original SMB analytical model can be extended to recreate moment reacting behaviour at the MB. It is worth considering the practicalities of this approach given that determining torsional spring stiffness values requires access to an FE model. Two pertinent questions related to this are therefore: 1) If one requires an FE model in the first place, why cannot all analysis be undertaken using it instead of the simplified representations proposed here? 2) Is it practical to assume an FE model will be available in general? With respect to the first question there are two main considerations which imply simplified models will likely be necessary. First, as has been touched upon, analysis over large numbers of load-cases and/or turbines becomes infeasible for high complexity models due to processing power requirements. In addition, any MB load model which might be embedded within existing aeroelastic software would likewise need to be computationally efficient (e.g. see (Girsang et al., 2014)). Considering the second question, detailed FE models of the drivetrain will commonly be used as part of the wind turbine design process. However, such models may well not be owned by or accessible to the wind farm operator. Despite this, the required spring stiffness values for simplified representations could be requested from the designer/manufacturer given that required parameters are unlikely to be considered sensitive or proprietary. In addition, it may transpire that sensible spring stiffnesses can be identified which allow operators to select appropriate values based on drivetrain dimensions and geometry without requiring access to detailed models; this possibility will be explored in future work.

To be clear, the detailed and high quality models used in existing work and outlined in Section 2 will remain crucial to the study of MB loading and operational behaviour. Rather than seeking to compete with such models, it is instead suggested that there are important synergies. For example, broader studies using simplified models can be leveraged to identify specific load cases requiring more detailed investigation with higher complexity models. Similarly, the MB load outputs of simple representations, obtained from coupling with aeroleastic code, can be used as inputs to more detailed models of bearing internal and external structure, allowing detailed studies to take place while preserving a level of modularity.

8 Conclusions

~~This paper has considered the validity of simplified analytical wind turbine drivetrain models for system analysis by comparing them with higher fidelity~~ This paper considers the question: Can analytical models be used to effectively evaluate load reactions for 3D ~~FE models.~~ main-bearing support configurations with either moment reacting or non-moment reacting behaviours? The results of ~~the comparison~~ comparisons with 3D FE drivetrain models, designed to exhibit the relevant load reaction properties, indicate that the existing ~~analytical models~~ single main-bearing analytical model can well represent bearing reaction forces ~~for bearingswhich do not react moments, while also showing it to not be suitable~~ in the non-moment reacting case (e.g. double row spherical roller bearings). However, it was also shown to be unsuitable for cases where a ~~bearing~~ support has moment reacting capabilities ~~.~~ (e.g. double row tapered roller bearings). Therefore, a second analytical model was created, through the addition of torsional springs, to represent a bearing ~~with moment reactions. Spring stiffness's~~ which supports moments as well as forces. Spring stiffnesses were found for this model using a static analysis of the FE model. Outputs from the new ~~model was~~ analytical model were compared with the moment reacting 3D model, with results indicating that it offers a greatly improved tool for analysis in the moment reacting case. The developed model was then used to consider mean and peak forces and moment reactions for this type of bearing across a range of operating conditions. ~~Future work on developing these models will be to consider how such reaction loading and moments properties will manifest within the bearing housing and on the rollers themselves for the two types of bearing which have been modelled thus far.~~

Appendix A: Input Output Table

Table A1 contains example input and output values for all models used in this work.

Table A1. Hub loading inputs and corresponding model outputs at various time steps. Quantities are in the DNV-GL Bladed reference frame.

Hub loading input						Output reaction forces	
My (Nm)	Mz (Nm)	Fx (N)	Fy (N)	Fz (N)	**Model**	Fy (N)	Fz (N)
967552	-233426	268017	-8425.5	-319983	Analytical DSRB	-73928	212450
					FE DSRB	-76192	209500
					Analytical DTRB	-18735	318080
					FE DTRB	-18384	314530
1077000	-10570	253819	-15968	-314370	Analytical DSRB	25024	160380
					FE DSRB	25273	154970
					Analytical DTRB	18955	285960
					FE DTRB	19191	283410
822305	776455	217225	-8469.5	-330719	Analytical DSRB	312340	287540
					FE DSRB	320690	286350
					Analytical DTRB	108690	365530
					FE DTRB	108420	362680

Appendix B: Shaft Sensitivity Analysis

A shaft sensitivity analysis was carried out to explore the effect of shaft thickness, and therefore stiffness, on the MB reaction force results for each model. The implemented models are assumed to have solid shafts, however, main shafts typically have small bore holes throughout the centre to allow for the passing of electrical cables. Therefore, thicknesses of 100%, 75% and 50% were compared to conservatively cover typical main shaft thicknesses and ensure the solid-shaft assumption does not impact the results of this work. Results are plotted below for the analytical DTRB, FE DSRB and FE DTRB models respectively. These results, in which only very small deviations can be seen, indicate that shaft thickness appears to have a minimal effect on model accuracy.

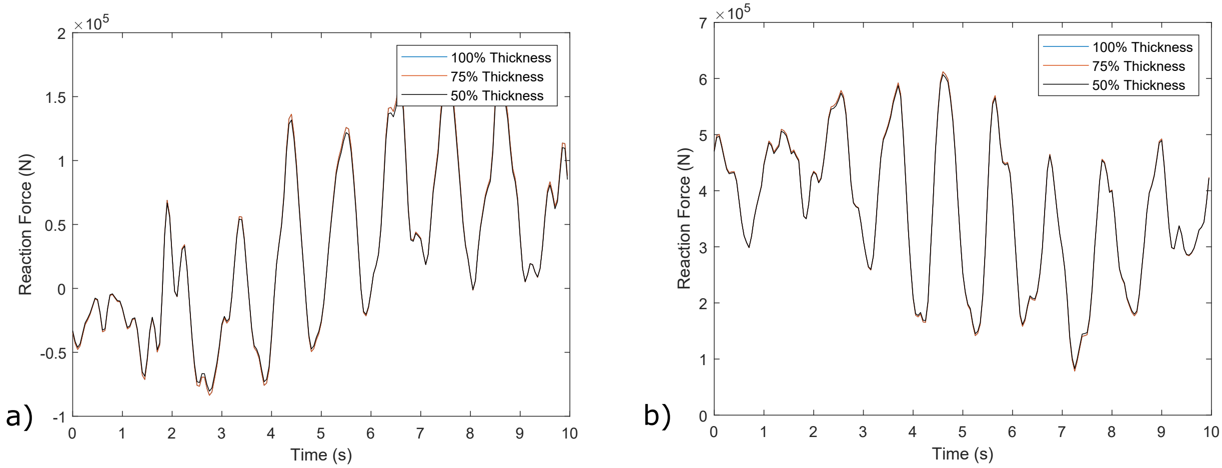

Figure B1. (a) Example time series of reaction force results in the horizontal plane from the analytical DTRB (with torsional springs) model when the shaft thickness is altered. (b) Example time series of reaction force results in the vertical plane from analytical DTRB (with torsional springs) model when the shaft thickness is altered.

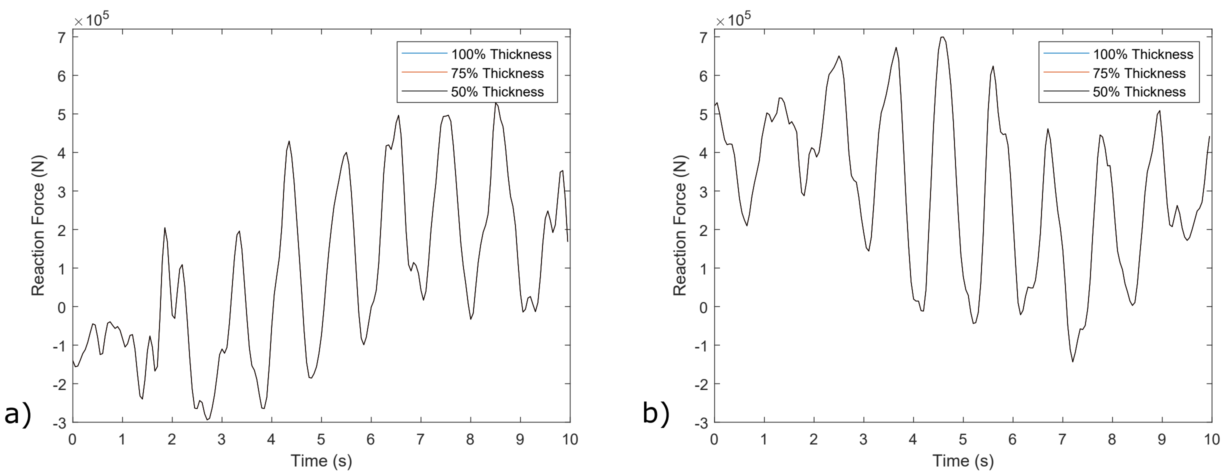

Figure B2. (a) Example time series of reaction force results in the horizontal plane from the FE DSRB model when the shaft thickness is altered. (b) Example time series of reaction force results in the vertical plane from the FE DSRB model when the shaft thickness is altered.

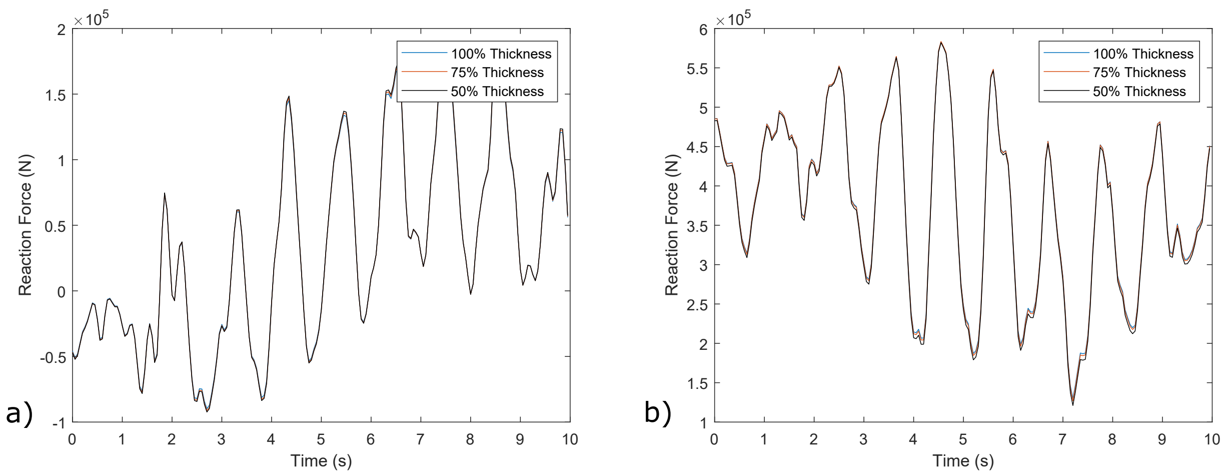

Figure B3. (a) Example time series of reaction force results in the horizontal plane from the FE DTRB model when the shaft thickness is altered. (b) Example time series of reaction force results in the vertical plane from the FE DTRB model when the shaft thickness is altered.

Competing interests. The authors declare they have no competing interests.

Acknowledgements. The authors would like to acknowledge ~~support and advice~~ extensive support throughout this work from Onyx Insight, specifically Robin Elliott, Rhys Evans and Evgenia Golysheva. This work was funded by the EPSRC (EP/L016680/1).

References

Artigao, E., Martín-Martínez, S., Honrubia-Escribano, A., and Gómez-Lázaro, E.: Wind turbine reliability: A comprehensive review towards effective condition monitoring development, Applied Energy, 228, 1569–1583, https://doi.org/10.1016/j.apenergy.2018.07.037, 2018.

Bosmans, J., Blockmans, B., Croes, J., Vermaut, M., and Desmet, W.: 1D-3D Nesting: Embedding reduced order flexible multibody models in system-level wind turbine drivetrain models, in: Conference for Wind Power Drives, 2019.

Cardaun, M., Roscher, B., Schelenz, R., and Jacobs, G.: Analysis of wind-turbine main bearing loads due to constant yaw misalignments over a 20 years timespan, Energies, 12, https://doi.org/10.3390/en12091768, www.mdpi.com/journal/energies, 2019.

Dowson, D. and Higginson, G. R.: Elastohydrodynamic Lubrication - Chapter 12, vol. 23, Pergamon Press Ltd., 1977.

Girsang, I. P., Dhupia, J. S., Muljadi, E., Singh, M., and Pao, L. Y.: Gearbox and drivetrain models to study dynamic effects of modern wind turbines, IEEE Transactions on Industry Applications, 50, 3777–3786, https://doi.org/10.1109/TIA.2014.2321029, 2014.

Harris, T. A.: Essential Concepts of Bearing Technology, FIFTH EDITION, CRC Press, https://doi.org/10.1201/9781420006599, https://www.taylorfrancis.com/books/9781420006599, 2006.

Hart, E.: Developing a systematic approach to the analysis of time-varying main bearing loads for wind turbines, Wind Energy, pp. 1–16, https://doi.org/10.1002/we.2549, 2020.

Hart, E., Turnbull, A., Feuchtwang, J., McMillan, D., Golysheva, E., and Elliott, R.: Wind turbine main-bearing loading and wind field characteristics, Wind Energy, 22, 1534–1547, https://doi.org/10.1002/we.2386, https://onlinelibrary.wiley.com/doi/abs/10.1002/we.2386, 2019.

Hart, E., Clarke, B., Nicholas, G., Kazemi Amiri, A., Stirling, J., Carroll, J., Dwyer-Joyce, R., McDonald, A., and Long, H.: A review of wind turbine main bearings: Design, operation, modelling, damage mechanisms and fault detection, https://doi.org/10.5194/wes-5-105-2020, https://doi.org/10.5194/wes-5-105-2020, 2020.

Hibbeler, R.: Structural Analysis, Pearson Education, 2011.

IEC: Wind turbines – Part 1: Design requirements, Tech. rep., IEC, 2005.

Junginger, M., Faaij, A., and Turkenburg, W. C.: Cost Reduction Prospects for Offshore Wind Farms, Tech. Rep. 1, 2004.

K. Leet, C. Uang, A. G.: Fundamentals of Structural Analysis, McGraw Hill, 2011.

Keller, J., Sheng, S., Cottrell, A., and Greco, A.: Wind Turbine Drivetrain Seminar Reliability Tribology Collaborative: A Recap, Tech. Rep. August, 2016.

Kock, S., Jacobs, G., and Bosse, D.: Determination of Wind Turbine Main Bearing Load Distribution, in: Journal of Physics: Conference Series, vol. 1222, https://doi.org/10.1088/1742-6596/1222/1/012030, 2019.

Popov, E. P.: Engineering Mechanics of solids, Prentice-Hall Inc., 1990.

Sethuraman, L., Guo, Y., and Sheng, S.: Main Bearing Dynamics in Three-Point Suspension Drivetrains for Wind Turbines, American wind energy association windpower, pp. 18–21, 2015.

Sinha, Y. and Steel, J. A.: A progressive study into offshore wind farm maintenance optimisation using risk based failure analysis, https://doi.org/10.1016/j.rser.2014.10.087, 2015.

Smalley, J.: Turbine components: bearings, http://www.windpowerengineering.com/design/mechanical/turbine-components-bearings-brakes-generators-hydraulics-seals-towers/, 2015.

Tavner, P. J., Xiang, J., and Spinato, F.: Reliability analysis for wind turbines, Wind Energy, 10, 1–18, https://doi.org/10.1002/we.204, http://doi.wiley.com/10.1002/we.204, 2007.

Tibbits, P. A.: Fem simulation and life optimization of tandem roller thrust bearing, Proceedings of the ASME International Design Engineering Technical Conferences and Computers and Information in Engineering Conference - DETC2005, 3 A, 79–88, https://doi.org/10.1115/detc2005-84234, 2005.

UK Government: Contracts for Difference Second Allocation Round Results, Tech. Rep. September, UK Government, 2017.

Walford, C. A.: Wind Turbine Reliability: Understanding and Minimizing Wind Turbine Operation and Maintenance Costs, Tech. rep., Sandia National Laboratories, http://www.ntis.gov/help/ordermethods.asp?loc=7-4-0{#}online, 2006.

Wang, S., Nejad, A. R., Bachynski, E. E., and Moan, T.: Effects of bedplate flexibility on drivetrain dynamics: Case study of a 10 MW spar type floating wind turbine, Renewable Energy, 161, 808–824, https://doi.org/10.1016/j.renene.2020.07.148, https://linkinghub.elsevier.com/retrieve/pii/S0960148120312246, 2020a.

Wang, S., Nejad, A. R., and Moan, T.: On design, modelling, and analysis of a 10-MW medium-speed drivetrain for offshore wind turbines, Wind Energy, 23, 1099–1117, https://doi.org/10.1002/we.2476, https://onlinelibrary.wiley.com/doi/abs/10.1002/we.2476, 2020b.

Wilkinson, M.: Measuring Wind Turbine Reliability-Results of the Reliawind Project, Tech. rep., https://doi.org/10.11333/jwea.35.2_102, 2011.

Wind Europe: Wind Energy in Europe in 2019, Tech. rep., Wind Europe, https://windeurope.org/wp-content/uploads/files/about-wind/statistics/WindEurope-Annual-Statistics-2019.pdf, 2020.

Yagi, S.: Bearings for Wind Turbine, NTN Technical review, 71, 40–47, 2004.